Highly anisotropic electron transport in shallow InGaAs heterostructures

S. Löhr,* S. Mendach, T. Vonau, Ch. Heyn, and W. Hansen
Institut für Angewandte Physik, Universität Hamburg, Jungiusstraße 11, D-20355 Hamburg, Germany
(Received 17 September 2002; published 14 January 2003)

We observe strikingly different magnetoconductivities in the two orthogonal ⟨110⟩ directions in strain relaxed $In_{0.75}Ga_{0.25}As/In_{0.75}Al_{0.25}As$ heterostructures on GaAs with an additional strained InAs channel. Up to 19% higher mobilities are found in the [-110] direction compared with the [110] direction. In addition, the [110] direction shows a pronounced positive parabolic magnetoresistance, which is not observed in [-110]. The degree of this anisotropic transport is found to decrease for an increase in electron density as well as for an increasing distance between the two-dimensional electron gas and the heterostructure surface. The positive magnetoresistance in [110] can be explained by the semiclassical theory on modulated two-dimensional electron gases. We tentatively attribute the potential modulation to anisotropic spatial variations in residual strain, which are correlated with the cross hatch morphology of the sample surface.

DOI: 10.1103/PhysRevB.67.045309 PACS number(s): 73.43.Qt, 73.63.Hs, 73.61.Ey, 81.07.St

The development of lattice-mismatched epitaxy of III-V semiconductor alloys, such as $In_xGa_{1-x}As$ and $In_xAl_{1-x}As$, on GaAs and InP substrates offers promising aspects for the design of electronic devices. However, the lattice mismatch between different layers can only be compensated for by elastic strain if the layer thicknesses do not exceed a critical value.[1] For thicker layers strain relaxation generally takes place via the formation of misfit and associated threading dislocations,[1] which degrade the electronic properties of the devices.[2] The strain fields associated with the misfit dislocations lead to the characteristic cross-hatch morphology,[3] which occurs in the form of trenches and ridges aligned along the two orthogonal in-plane ⟨110⟩ directions at the heterostructure surface.[4,5] For strain-relaxed SiGe films grown on Si, it has been shown that the cross-hatch morphology is highly correlated with large lateral variations in the surface strain.[6] Studies of the strain relaxation in step-graded $In_xGa_{1-x}As$/GaAs heterostructures revealed spatial variations of the in-plane strain.[7] Due to the lack of inversion symmetry in III-V semiconductors, orthogonal directions are not equivalent, which affects the uniformity of the strain relaxation and the epitaxial growth.[8,9] Anisotropic transport-properties of two-dimensional electron gases (2DEGs) in heterostructures containing strained or strain relaxed layers have been reported by several authors. [9–13] These anisotropies were associated with asymmetric lattice defects and/or surface morphologies. Anisotropic ordering effects during strained-layer epitaxial growth were also reported.[11] However, complete correlations between asymmetric structural and electronic properties are not clear at present.

In this work, we report on highly anisotropic magnetotransport properties of modulation-doped $In_{0.75}Ga_{0.25}As/In_{0.75}Al_{0.25}As$ heterostructures embedding an additional strained InAs channel grown on GaAs. In addition to a mobility anisotropy along the two orthogonal ⟨110⟩ directions of up to 19%, the low-mobility direction [110] shows a pronounced positive parabolic magnetoresistance, which is not observed in [-110]. We show that this positive magnetoresistance can be explained by a weak potential modulation resulting in a spatially varying electron density. The origin of the potential modulation is tentatively attributed to anisotropic spatial variations in residual strain. The dependence of the anisotropic electron transport on the distance between the 2DEG and the heterostructure surface together with atomic force microscopy studies of the surface suggest a correlation between the anisotropic transport properties and the asymmetric cross-hatch morphology.

The samples are grown by molecular-beam epitaxy on a (001) GaAs substrate. For strain relaxation a step graded buffer consisting of six 100-nm-thick layers of $In_xAl_{1-x}As$ with increasing indium content is grown. The specific growth details are reported in previous publications.[2,13] The buffer layer is followed by an $In_{0.75}Al_{0.25}As$ layer doped within 7 nm and a subsequent undoped spacer layer of 5-nm thickness. The channel containing the 2DEG consists of a 16-nm $In_{0.75}Ga_{0.25}As$ quantum well with an asymmetrically inserted 4-nm InAs layer. The whole structure is capped by an $In_{0.75}Al_{0.25}As$ layer. Using this template we have grown three different samples with cap thicknesses of 6, 16, and 36 nm. Shubnikov-de Haas (SdH) and Hall measurements are carried out on photolithographically defined L-shaped Hall bars with a width of 100 μm and a length to width ratio of 4, aligned along the two orthogonal in-plane directions [110] and [-110]. The measurements are performed at a temperature of 4.2 K. The signals are detected using lock-in technique and a current of 0.1 μA. To assess the mobility as a function of the carrier density we illuminate the samples with a red light-emitting diode resulting in an increase of the electron density.

Table I shows the intrinsic, i.e., before illumination of the samples, electron mobilities μ and densities N_s for the three samples. The samples show only slightly different densities which could be due to the different cap thickness influencing the charge distribution in the heterostructures. A much smaller difference in the density is also found between the orthogonal ⟨110⟩ directions, which is comparable to the density deviations measured between different voltage probes of a Hall bar oriented along only one crystal direction. Comparing the mobilities in the two ⟨110⟩ directions we observe a mobility anisotropy, which is as high as 19% for the most shallow sample. For the less shallow structures this anisotropy decreases gradually. Moreover, we find that the mobil-

 ©2003 The American Physical Society

TABLE I. Electron densities and mobilities in the two ⟨110⟩ directions for the three samples with different distances between the 2DEG and the surface.

Cap thickness	[-110] N_s (10^{11} cm^{-2})	[-110] μ (cm^2/V s)	[110] N_s (10^{11} cm^{-2})	[110] μ (cm^2/V s)
6 nm	4.2	100 000	4.1	81 000
16 nm	4.0	100 000	3.9	90 000
36 nm	3.8	98 000	3.8	93 000

ity anisotropy decreases for increasing electron density. The low-mobility [110] direction shows an undulation period of the cross-hatch morphology which is about four times shorter than that in the [-110] direction. Figure 1 shows an atomic force microscopy (AFM) image of the 36-nm cap sample surface visualizing the cross hatch pattern. The height variations are in the 10–20-nm regime. The fast Fourier transform of the AFM image [Fig. 1(b)] clearly shows periodicities of the cross-hatch pattern in the [-110] and [110] directions with periods of $a \sim 5.5$ and 1.3 nm, respectively.

In addition to the mobility anisotropy, we find strikingly different magnetoresistivities in the orthogonal ⟨110⟩ directions, which is shown in Figs. 2(a) and 2(b). Comparing the resistance curves in the two directions, a pronounced positive parabolic magnetoresistance is observed in [110], but not in [-110]. For magnetic fields $B > 1$ T this positive magnetoresistance is superimposed by the emerging SdH-oscillations, which further are much higher in amplitude in [110] than in [-110]. The differences in the magnetoresistivity curves become stronger for decreasing distance between the 2DEG and the surface, as can be seen directly from Figs. 2(a) and 2(b). As for the mobility anisotropy, these differences decrease gradually at higher electron densities. For the 36-nm cap sample no difference in the magnetoresistivities is found for a density of $N_s \sim 6.0 \times 10^{11}$ cm^{-2}. This is demonstrated in Fig. 2(c) where both traces are nearly identical and almost no mobility anisotropy is found.

We would like to note that in both directions the SdH oscillation minima reach zero for magnetic fields above 4 T. Furthermore, the carrier densities determined from SdH and Hall measurements agree within less than 2%. These findings

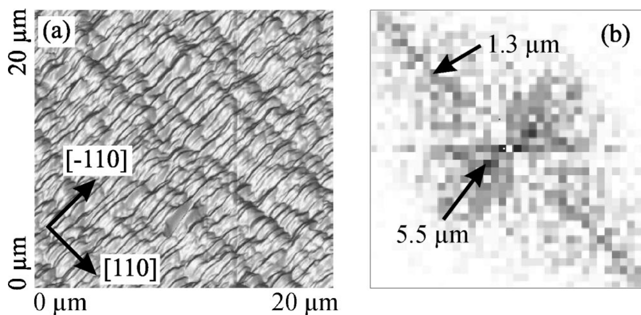

FIG. 1. AFM image (a) revealing the cross-hatch morphology of the surface for the 36-nm cap sample. The fast Fourier transform (b) clearly shows different periodicities in the two ⟨110⟩ directions.

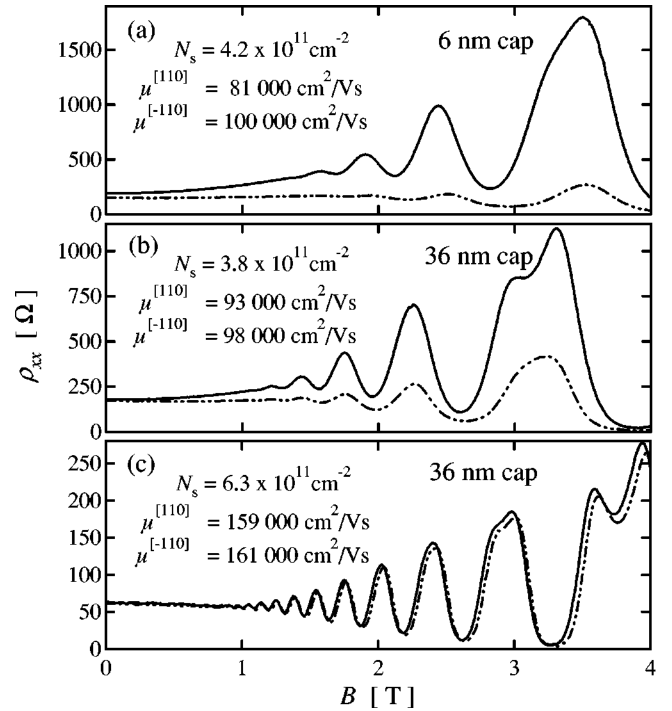

FIG. 2. Anisotropic magnetoresistances in the [−110] (dashed curves) and [110] (solid curves) directions of the 6-nm cap (a) and the 36-nm cap (b) samples. In addition to the mobility anisotropy, a strong positive magnetoresistance is observed in [110], which disappears for higher electron densities (c).

indicate that there is no parallel conduction in our samples, and we can exclude this effect as an explanation for the positive magnetoresistance.

A positive magnetoresistance has been observed in periodically modulated 2DEGs at high magnetic fields, where the cyclotron radius r_c is much smaller than the period a of the density modulation.[14] It has been found that this nonoscillatory magnetoresistance arises beyond the low-field commensurability oscillations,[15,16] and follows directly from the theory by Beenakker.[17] Originally, Beenakker derived a semiclassical expression for a weak potential modulation explaining the commensurability oscillations in terms of a resonance between the periodic cyclotron motion and the oscillating $\boldsymbol{E} \times \boldsymbol{B}$ drift of the orbit center induced by the modulation. For $\omega_c \tau \gg 1$ and a modulation strength $\varepsilon \equiv eV_{\rm rms}/E_F \ll 1$ the longitudinal magnetoresistivity is given by[17]

$$\rho_{xx}/\rho_0 = 1 + 0.5(\varepsilon q l)^2 J_0^2(q r_c)[1 - J_0^2(q r_c)]^{-1}, \qquad (1)$$

where $J_0(z)$ is the Bessel function of the first kind of order zero and real argument z, ω_c, and r_c are the cyclotron frequency and radius, respectively, τ is the electron scattering time, E_F is the Fermi energy, l is the mean free path, $q = 2\pi/a$, and the potential modulation is taken as $V(x) = \sqrt{2} V_{\rm rms} \sin(2\pi x/a)$. Assuming a weak modulation of the carrier density in [110] for our samples, it is likely to have a period similar to that of the cross hatches, we determine the modulation strength ε by fitting our magnetoresistance data with Eq. (1).

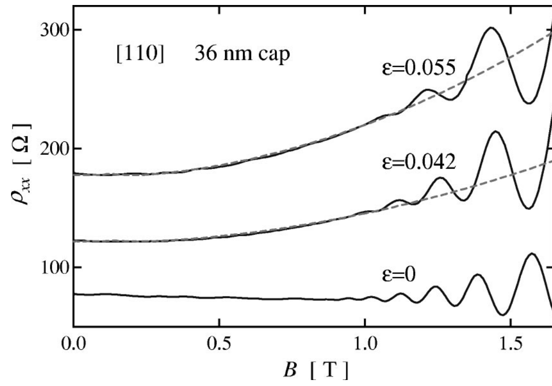

FIG. 3. A comparison between the measured magnetoresistances in [110] (solid curves) and the theoretical expression (dashed curves; see Eq. (1)) in the magnetic field range for which the positive magnetoresistance is not concealed by the SdH oscillations. A clear dependence of the determined modulation strength ε on the carrier density can be seen. The three curves correspond to carrier densities (from bottom to top): $N_s = 5.7/4.6/3.8 \times 10^{11}$ cm^{-2}.

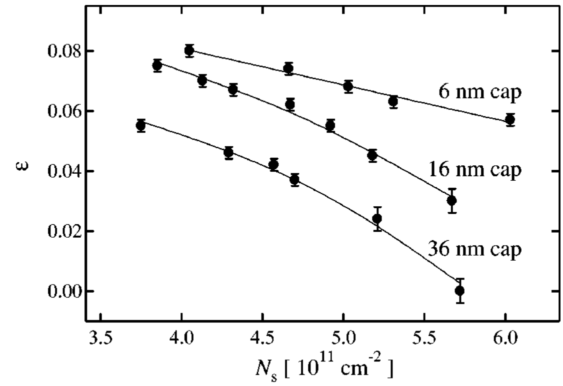

FIG. 4. Strength ε of the 2DEG modulation in dependence on the carrier density for the three samples with different distances between the 2DEG and the surface. The modulation strengths ε are determined as is described in the text. The lines are guides to the eye.

Figure 3 shows the magnetoresistances in [110] for three different carrier densities and the calculated fits using Eq. (1). The only adjustable parameter used for the fits is the modulation strength ε. The Fermi energy E_F and the mean free path l are determined directly from each magnetoresistance curve for each fit. The modulation period is assumed to be $a = 1.3$ μm, which is the undulation period determined for troughs orthogonal to [110] at the sample surface (see Fig. 1). We find a very good agreement between the experiment and the theoretical expression until the onset of the SdH-oscillations, which are not included in the theory. Slight deviations between the fits and experiment, which are hardly visible on the scale of Fig. 3, are not surprising since the theoretical assumption of a sinusoidal modulation of the electron density will differ from the experimental situation. The determined modulation strengths ε are of the order of a few percent, which agrees with other experiments on weakly modulated 2DEGs.[14–16] Moreover, we note that the positive magnetoresistance is not influenced by temperatures of up to 25 K, which indicates that we are dealing with a classical transport phenomenon. The commensurability oscillations periodic in $1/B$ are not observed in the experiment, and are too small to be resolved in the calculated traces in Fig. 3. They would occur at fields at which $2r_c > a$. At these fields the commensurability oscillations cannot be observed in our relatively low-mobility samples, since the condition $\mu B \gg 1$ does not hold.[17]

Figure 4 shows the modulation strength ε determined for all three samples as a function of the carrier density. Qualitatively the modulation strength ε behaves as expected from the density dependence and the cap layer dependence of the anisotropy. For each sample we find a monotonic decrease of ε with increasing carrier density. If we assume the potential modulation eV_{rms} to be an intrinsic property of the crystal structure, i.e., constant, a higher carrier density results in a weaker modulation $\varepsilon \equiv eV_{rms}/E_F$ of the 2DEG. Furthermore, the modulation strength ε decreases for increasing distance between the 2DEG and the crystal surface. At high densities the modulation vanishes for the 36-nm cap sample, whereas it is still present for the more shallow structures (compare Fig. 2). Apart from an offset, the density dependencies of ε in the 16-nm and 36-nm cap samples are identical. The reason for the slightly different behavior of the 6-nm cap sample in comparison with the 16-nm and 36-nm cap samples for higher densities is not clear to us at present.

We tentatively attribute a potential modulation to spatial variations of the residual in-plane strain. For strained SiGe films on Si the existence of laterally varying strain fields and its correlation with the cross-hatch morphology has been demonstrated.[6] Anisotropic in-plane strain relaxation is also reported for $In_xGa_{1-x}As/GaAs$ heterostructures, resulting in μm-scale variations of uniaxial and biaxial strains.[7–9] The hydrostatic strain components directly influence the band lineup of the heterostructure[18] and could thus lead to a potential fluctuation interacting with the 2DEG. Nonhydrostatic strain (shear strain) is known to affect the electronic structure by removing band degeneracy. An additional contribution may result from piezoelectric effects, which couple to shear stresses.[9,19] The fact that a positive magnetoresistance is only observed in one of the two $\langle 110 \rangle$ directions as well as the observed mobility anisotropy may at least be partly due to an anisotropic strain relaxation concomitant with an asymmetric misfit dislocation density.[2] The systematic dependence of the modulation strength ε on the shallowness of the sample, i.e., on the distance between the 2DEG and the crystal surface, indicates that the anisotropic transport properties are closely related to the asymmetric cross-hatch morphology. Assuming the potential modulation to arise from residual strain, we roughly estimate the average residual strain, i.e., the average residual lattice mismatch. We use a deformation potential of 5.6 eV by interpolating between the values given for InAs and GaAs.[18] For the 6-nm cap sample with $\varepsilon = 0.08$ this would yield a residual lattice mismatch of $\sim 0.04\%$. Taking into account the simplicity of this estimate, i.e., especially the negligence of the screening of the 2DEG, this value is in good agreement with results from direct measurements of the residual strain.[6–8]

In summary, we report on highly anisotropic magne-

totransport properties of shallow modulation-doped $In_{0.75}Ga_{0.25}As/In_{0.75}Al_{0.25}As$ heterostructures containing an additional strained InAs channel grown on GaAs. We find a mobility anisotropy of up to 19% in the two orthogonal ⟨110⟩ directions. The low-mobility direction [110] shows a positive magnetoresistance. Both the mobility anisotropy and the positive magnetoresistance decrease for increasing electron density as well as for an increase of the distance between the 2DEG and the sample surface. This positive magnetoresistance can be understood in terms of a modulated electron density in [110]. The origin of the potential modulation is tentatively attributed to anisotropic spatial variations in residual strain, which are correlated with the cross-hatch morphology of the sample surface.

We wish to thank T. Maltezopoules for performing the AFM images, and the Deutsche Forschungsgemeinschaft for financial support via the Sonderforschungsbereich 508 "Quantenmaterialien".

*Electronic address: sloehr@physnet.uni-hamburg.de

[1] J. W. Matthews and A. E. Blakeslee, J. Cryst. Growth **27**, 118 (1974).
[2] S. Mendach, C. M. Hu, Ch. Heyn, S. Schnüll, H. P. Oepen, R. Anton, and W. Hansen, Physica E (Amsterdam) **13**, 1204 (2002).
[3] E. A. Fitzgerald, Y.-H. Xie, D. Monroe, P. J. Silverman, J. M. Kuo, A. R. Kortan, F. A. Thiel, and B. E. Weir, J. Vac. Sci. Technol. B **10**, 1807 (1992).
[4] E. A. Fitzgerald, D. G. Ast, P. D. Krishna, G. D. Pettit, and J. M. Woodall, J. Appl. Phys. **63**, 693 (1988).
[5] K. H. Chang, R. Gibala, D. J. Srolovitz, P. K. Bhattacharya, and J. F. Mansfield, J. Appl. Phys. **67**, 4093 (1990).
[6] D. E. Jones, J. P. Pelz, Y. Hong, I. S. T. Tsong, Y.-H. Xie, and P. J. Silverman, Appl. Phys. Lett. **69**, 3245 (1996).
[7] K. Rammohan, D. H. Rich, R. S. Goldman, J. Chen, H. H. Wieder, and K. L. Kavanagh, Appl. Phys. Lett. **66**, 869 (1995).
[8] J. C. P. Chang, J. Chen, J. M. Fernandez, H. H. Wieder, and K. L. Kavanagh, Appl. Phys. Lett. **60**, 1129 (1992).
[9] R. S. Goldman, H. H. Wieder, K. L. Kavanagh, K. Rammohan, and D. H. Rich, Appl. Phys. Lett. **65**, 1424 (1994).
[10] T. Schweizer, K. Köhler, W. Rothemund, and P. Ganser, Appl. Phys. Lett. **59**, 2736 (1991).
[11] P. Ramvall, N. Carlsson, P. Omling, L. Samuelson, W. Seifert, M. Stolze, and Q. Wang, Appl. Phys. Lett. **68**, 1111 (1996).
[12] S. Gozu, T. Kita, Y. Sato, S. Yamada, and M. Tomizawa, J. Cryst. Growth **227-228**, 155 (2001).
[13] A. Richter, M. Koch, T. Matsuyama, Ch. Heyn, and U. Merkt, Appl. Phys. Lett. **77**, 3227 (2000).
[14] A. K. Geim, R. Taboryski, A. Kristensen, S. V. Dubonos, and P. E. Lindelof, Phys. Rev. B **46**, 4324 (1992).
[15] D. Weiss, K. v. Klitzing, K. Ploog, and G. Weimann, Europhys. Lett. **8**, 179 (1989).
[16] R. W. Winkler, J. P. Kotthaus, and K. Ploog, Phys. Rev. Lett. **62**, 1177 (1989).
[17] C. W. J. Beenakker, Phys. Rev. Lett. **62**, 2020 (1989).
[18] C. G. Van de Walle, Phys. Rev. B **39**, 1871 (1989).
[19] I. A. Larkin, J. H. Davies, A. R. Long, and R. Cuscó, Phys. Rev. B **56**, 15 242 (1997).